Journal of Analytical and Applied Pyrolysis 109 (2014) 159–167

Contents lists available at ScienceDirect

Journal of Analytical and Applied Pyrolysis

journal homepage: www.elsevier.com/locate/jaap

Generalized model of n-heptane pyrolysis and steam cracking kinetics based on automated reaction network generation

Petr Zámostný[a,*], Adam Karaba[a,c], Natália Olahová[b], Jiří Petrů[a,c], Jan Patera[a], Elena Hájeková[b], Martin Bajus[b], Zdeněk Bělohlav[a]

[a] Institute of Chemical Technology Prague, Faculty of Chemical Technology, Department of Organic Technology, Technická 5, CZ-166 28 Praha 6, Czech Republic
[b] Slovak University of Technology, Faculty of Chemical and Food Technology, Institute of Organic Chemistry, Catalysis and Petrochemistry, Department of Petroleum Technology and Petrochemistry, Radlinského 9, SK-812 37 Bratislava, Slovak Republic
[c] Research Institute of Inorganic Chemistry, Revolucni 1521/84, 400 01 Usti nad Labem, Czech Republic

ARTICLE INFO

Article history:
Received 6 March 2014
Accepted 29 June 2014
Available online 15 July 2014

Keywords:
n-Heptane
Pyrolysis
Steam cracking
Kinetic model
Reaction network generation

ABSTRACT

Mathematical model of n-heptane pyrolysis under thermal cracking and steam cracking conditions was developed. The objective was achieving good generalization by combining two different data sources for model identification. The data sources included experimental pyrolysis data for many structurally different hydrocarbons measured at reference conditions as well as the data for n-heptane measured in different reactors at different reaction conditions. The model was developed using the automated reaction network generation. The generated network included hydrogen abstraction, β-scission, radical isomerization and recombination reactions, the kinetic parameters of which were expressed as functions of 26 group contribution factors. Molecular reactions and radical additions were substituted by 12 formal shortcut molecular reactions. The initial values of kinetic parameters and group contribution factors were adopted from previous study, where they were obtained by regression based on the experimental data involving wide range of linear, branched and/or cyclic hydrocarbons. More experimental data on n-heptane pyrolysis measured under different conditions, including the use of two different reactors, were added to the data set used for the parameter optimization. The model simulations showed good agreement with the experimental data even for the validation samples. Thus, the proposed approach proved the ability to produce models achieving good generalization.

1. Introduction

Steam-cracking is one of the fundamental and the most important processes in the petroleum processing industry, aimed at producing light olefins, such as ethylene, propylene, butenes and aromatics. The process is based on the thermal non-catalyzed decomposition of various hydrocarbon feedstocks by pyrolysis reactions. The feedstock quality and the processing parameters have a great potential impact on the economy of the process. Previously, we developed a mathematical model of steam-cracking process [1], which has been successfully used in the industrial practice [2–6]. In order to further improve the model capabilities, there is a long-term objective of replacing the included semi-mechanistic kinetic model by a one based on mechanistic approach.

Mathematical models of steam-cracking can be divided between empirical and mechanistic ones. Empirical models [7,8] often rely on simplifying the complex network of radical reactions by substitute molecular reactions. They can describe the experimental data very well within the experimental region, but due to the substitute nature of the kinetic parameters used, they generalize not as well as the more mechanistic approaches. Thus, the possibility of extrapolating results to the different piece of equipment is very limited. Mechanistic models based on the kinetic description of the radical mechanism do not have this kind of disadvantage, as they are usually much more complex, even for very simple feedstocks.

Mechanistic models were initially designed specifically for a single feedstock molecule (or a single type of molecule), such as the one developed by Sundaram and Froment [9,10], who were interested in the development of the mechanistic model describing the thermal cracking of butanes. A fully integrated mechanistic model was firstly published later by Allara and Shaw [11]. They published the complete system of free-radical chemical reactions (elementary

* Corresponding author. Tel.: +420 2 20444222.
E-mail address: petr.zamostny@vscht.cz (P. Zámostný).

http://dx.doi.org/10.1016/j.jaap.2014.06.017
0165-2370/

steps) together with recommended values of kinetic parameters supplemented by values obtained by other authors. Mechanistic modeling continued by careful investigation of assumptions that were initially made without positive prove such as the differences between 1D and 2D model of steam-cracking tubular reactor [12]. Other authors created models for more complex feedstock molecules [13,14], tested significance of several reactions pathways and compared their results with previously known literature data.

As increasingly more variable feedstocks started being processed by the industry, it requires steam-cracking models to become more flexible. Designing the mechanistic model "manually" becomes very time-consuming process, prone to many errors and inconsistencies, hence more complex approaches were employed. Primary pyrolysis reactions can be described by relatively simple set of general kinetic rules and the automated reactions network generation (RNG) became a new standard practice. One of the first tools that could be used for this purpose was published by Di and Lignola [15] under the name KING (Kinetic Network Generator). Other authors [16,17] were interested in developing similar tools for mechanism generation and its application for steam-cracking of ethane.

There are several papers aimed at using RNG for modeling of steam-cracking of more complex individual components as feedstock. Van Geem et al. [18,19] utilized this approach for modeling of n-hexane. Using this kind of model, it was possible to investigate in details original assumptions such as QSSA (Quasi steady state species) or μ-hypothesis [20,21] or significance of pressure-dependent kinetic parameters [22,23].

Another task in steam-cracking modeling is to find a reliable source of kinetic parameter values. An interesting approach shared by several groups of authors [8,22,24,25] involves determining the kinetic parameters by ab initio calculations or similar tools of computational chemistry. In order to reduce number of necessary parameters, some authors follow the path of reducing the reaction mechanism. Permual et al. [26] developed a method allowing the simplification of reaction mechanism based on dynamic sensitivities analysis and used it in their pyrolysis and combustion model. Huang [27] presented a reduction method based on sensitivity and principal component analysis and demonstrated its properties on example of its application to a methane-rich fuel consumption model. Edwards, Androulakis, and Mitsos [28–30] used reduction methods based on linear or non-linear programming, solving the model reduction as a constrained optimization problem, the elimination of species and/or reactions being done, so as to produce the simplest model with an acceptable model reduction error.

Another approach is calculating the parameters using the group-contribution and bond additivity methods, like the one developed by Benson [31]. The exact implementation may focus either on greater detail of the specific type of radical reactions description [32], or the substantial reduction of the number of kinetic parameters [33].

The comparison provided above shows the automated RNG approach is superior, but the authors focus more on the aspect of developing extremely detailed models of single compound cracking, rather than universal model modeling the cracking of arbitrary hydrocarbon, which would be more suitable for development of industrial steam-cracking models. Most authors also find necessary to adjust the kinetic parameters to fit the experimental data, because the kinetic parameters of the complex reaction networks are inter-correlated and it is hard to combine parameters obtained from different sources. The models are typically tailored to one system, usually describing only one type of feedstock.

Thus, our preceding work was primarily aimed at the development of the radical mechanistic model using automated RNG and the group contribution method for kinetic parameters estimation [34,35]. Optimizing the relatively few group-contribution factors improved the model generalization, so that it is able to simulate substantially different feedstock types (n-alkanes, i-alkanes, cycloalkanes) and their behavior in the micro-pyrolysis reactor [36] at varied temperature (650–815 °C) and residence time (0.1–1.0 s). The next step in our effort for improved model generalization was to extend the model to simulating the pyrolysis experiments in two substantially different reactors, using only one shared set of generalized kinetic parameters, represented by group contribution factors. At the same time, the model ability to simulate pyrolysis of different structures, using the one generalized set of parameters, should be maintained.

While our approach included using the experimental data for more hydrocarbons [37], one compound had to be chosen as the key model substance. In the group of alkanes C_5H_{12} to $C_{12}H_{26}$ at about 780 °C, n-heptane gives the highest conversion and the highest yield of ethylene [38]. Therefore, n-heptane is particularly suitable for studies of kinetics and mechanisms of pyrolysis at different reaction rates, and in reaction systems [39,40]. Our previous work dealt with the study of pyrolysis of C_7 – hydrocarbons in the presence of steam in a flow reactor. Thus, in this study, n-heptane was selected as a key model feedstock because it is an excellent model compound for studying the cracking behavior of heavy naphtha fraction (90–180 °C). The kinetics of heptane pyrolysis is somewhat more complex than that of hexane reported previously [19], due to longer hydrocarbon chain and thus more opportunities for radical isomerization.

Several research groups published fundamental studies of n-heptane pyrolysis [7,41–48]. Appleby et al. [41] and Chakraborty [48] carried out the pyrolysis at high pressure. They supposed that the yields of ethane and propane increase with increasing pressure while the yield of ethylene decreases. Bajus et al. [45] investigated the pyrolysis of n-heptane in flow reactor at atmospheric pressure with the steam as inert. The pyrolysis at atmospheric pressure was also studied by Murata and Saito [42–44] and they also proposed the molecular model for the product distribution. Aribike and Susu [46,47] developed mechanistic model of n-heptane pyrolysis using the kinetic description of radical decomposition. They showed the mechanistic model is able to describe the behavior of n-heptane satisfactorily even under various experimental conditions (740-780 °C, 0.7-1.0 s residence time).

2. Experimental

The experimental data used in this work were obtained on two different reactors and experimental setups used by two co-operating research groups. Reactor A is a micro-reactor operated in a pulse regime, on-line connected to a multi-column system for detailed product separation by gas chromatography. A feedstock is introduced into the reactor in the liquid state into the stream of a nitrogen carrier gas. It is very quickly vaporized, so that a pulse of reaction mixture is formed, passes through the reactor non-diluted, and proceeds to the chromatograph analysis immediately after the reaction. The most important reactor characteristics are provided in Table 1 and more detail of the experimental method can be found elsewhere [49]. The key feature of the reactor A is very rapid operation and sample flexibility, that allowed an extensive set of pyrolysis data for a broad variety of hydrocarbon species to be measured [36]. Therefore, there is a substantial data base representing the effects of hydrocarbon structure variability on pyrolysis reactions. On the other hand, the micro-size of the reactor is also its most significant drawback. The temperature profile is determined somewhat less accurately along a very short reactor length and there may be some systematic error in the results. However, the sensitivity to structure variability is maintained and the data from

Table 1
Properties of pyrolysis reactors A and B used for obtaining the experimental data.

	Reactor A [30]	Reactor B [32]
Mode of operation	Pulse	Continuous
Inlet pressure, kPa	400	101
Dilution media	None	Steam
Length, mm	120	750
Modeled length, mm	75	300
Inner diameter, mm	4.0	12.0/6.0 (outer/inner tube)
Effective inner diameter, mm	4.0	10.4
Material	Quartz	Steel (CS Standard 17255)
Filler (material, porosity)	Silicon carbide, 0.4	None

reactor A are the valuable source for supplying the information on the structural behavior of different hydrocarbons.

There comes the advantage of using the data [40] from another reactor (Reactor B, see Table 1), which is substantially made from stainless steel (Czechoslovak standard 17255; 23-27% Cr, 18-22% Ni, max. 2% Si, max. 1.5% Mn, max. 0.25% C). The reactor is operated in continuous mode using the hydrocarbon dilution by steam. The temperature profile is observed by moving thermocouples (Ni/Cr–Ni) placed in the inner tube placed co-axially within the reactor tube. The reactants (hydrocarbon and water) are transported from the glass burettes by micro-pumps into the pre-heater where they are evaporated and then the feed flows through a connecting tube into the reactor. After the reaction, the pyrolysis products flow through a water cooler and they are cooled in a freezing trap. The detailed description of the pyrolysis reactor is given in [50]. Gas chromatography is used for the analysis of gaseous and liquid products [51]. The main strength of the apparatus is the possibility for a very accurate measurement of the temperature profiles, feed rates, as well as using different steam dilution ratios, but the operation is more time consuming, hence obtaining a broad variety of experimental data in terms of the hydrocarbon structure would be very time consuming.

The reactors also differ in their maximum operating temperature and their temperature profiles (Fig. 1). Most notably the reactor B operating temperature is limited to <760 °C. The inner

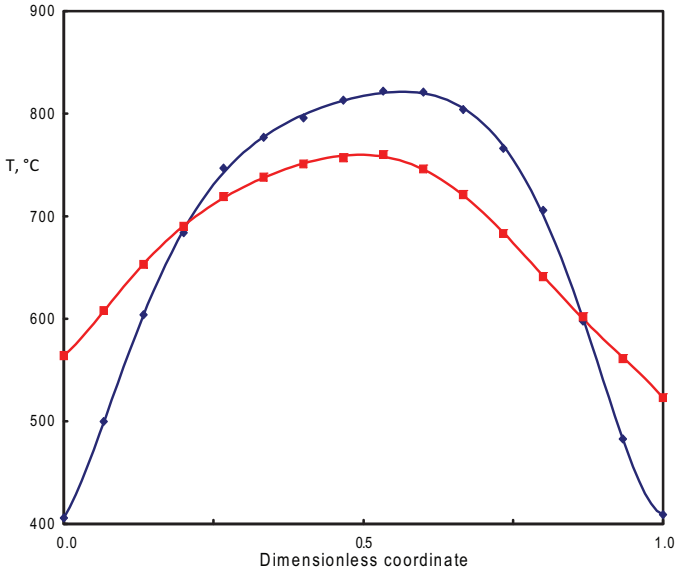

Fig. 1. Illustration of measured temperature profiles along the reactor A ◆ operated at peak temperature 810 °C, and continuous reactor B ■ operated at peak temperature 760 °C.

reactor surface-to-volume ratio is 6.65 cm^{-1}, which is high compared to industrial reactors. The wall effects become more apparent when the surface-to-volume ratio is increased at higher temperature (>760 °C). The deposition of coke on the wall of the reactor is a serious problem in the study, since coke is mainly deposited on the wall of the reactor there is a continuous change in the surface properties of the reactor. This results in a continuous change of the composition of the reaction products. On the other hand, reactor A is made of quartz and the operating temperature is limited only by the equipment design.

2.1. Mathematical model

The idea behind this work was taking the advantage of having the results of two different experimental methods for measuring the kinetics of pyrolysis reactions, combining their strengths and eliminating their weaknesses, in order to improve the generalization of the mathematical model of steam-cracking reaction kinetics.

The underlying mathematical model of hydrocarbon thermal cracking is based on the automated generation of reactions network (RNG) by the tool we have recently developed [34,35]. Generated reaction network involve typical primary pyrolysis reactions including:

- hydrogen abstraction by active radical,
- β-scission of radicals (C—C and C—H bonds scission),
- isomerization of radicals (1-4, 1-5 positions),
- isomerization of allyl-type radicals (switching the double bond and the unpaired electron position),
- termination of non-fissionable radicals (such as hydrogen, methyl, allyl if there is no other stabilization path), by hydrogen radical recombination.

Hydrogen abstraction reactions of a hydrogen atom by all possible radicals are lumped to a single reaction expressing the abstraction by “active radical”. The active radical activity is calculated as the sum of radical concentrations weighted by the relative rate of hydrogen abstraction by the respective radicals. Concentration of radicals are obtained using a pseudo-stationary principle, taking into account the rates of initiation and termination reactions as a functions of hydrocarbon mixture composition [34]. The effect of temperature and pressure on the pseudo-stationary concentrations is applied by standard thermodynamic calculations.

Kinetic parameters of involved reactions are determined according to the developed group contribution method. In this method, the reactions are lumped into reaction groups sharing the same structure near the reaction center and therefore also the base kinetic parameters. Those base parameters are modified if appropriate by further factors, reflecting the effects of structure elements on the reaction center reactivity. For example, hydrogen abstraction frequency factor is the same for each hydrogen atom in the molecule, but the activation energy depends on the type of carbon atom, which the hydrogen is bonded to. Therefore, there are three different factors representing the activation energy of hydrogen abstraction from primary, secondary, or tertiary carbon atom. Other group contribution factors, such as a decrement due to the presence of a double bond in the allylic position or an increment due to the presence of a double bond in the vinylic position, may also affect the resulting value of the activation energy parameter. In a similar manner, the β-scission reactions are lumped by the type of split bond and modified by factors representing the number of alkyl-substituents of the bond undergoing the scission. This lumping means there should be different parameters specific for:

Table 2
Group of reactions formally replacing radical addition, isomerization, scission and hydrogenation of light components.

Reactants		Products		A[a]	E, kJ mol^{-1}
C_2H_4	H_2	C_2H_6		2.8×10^{01}	50.6
C_4H_6	C_2H_4	C_6H_6	$2H_2$	5.5×10^{01}	20.4
C_4H_6	C_3H_6	CH_3-C_6H_5	$2H_2$	5.5×10^{01}	12.0
C_4H_6	1-C_4H_8	C_2H_5-C_6H_5	$2H_2$	5.5×10^{01}	0.0
C_4H_6	2-C_4H_8	o-Xylene	$2H_2$	5.5×10^{01}	0.5
C_4H_6	C_4H_6	C_2H_3-C_6H_5	$2H_2$	5.5×10^{01}	10.0
1-C_4H_8		2-C_4H_8		5.0×10^{05}	103.7
2-C_4H_8		1-C_4H_8		4.2×10^{06}	105.7
C_3H_6	H_2	CH_4	C_2H_4	1.7×10^{08}	179.6
1-C_4H_8	H[a]	1-C_4H_9[a]		2.4×10^{11}	2.0
2-C_4H_8	H[a]	2-C_4H_9[a]		2.4×10^{11}	3.0
i-C_4H_8		1-C_4H_8		1.5×10^{06}	99.6

[a] The frequency factor dimension depends on reaction molecularity (s^{-1} or $m^3\ mol^{-1}\ s^{-1}$).

– the C—H bond on primary, secondary, and tertiary carbon atom,
– the C—C bond with hydrogen atom(s), substituted by 1, 2, and 3–6 alkyls.

The influence of double bonds in β-position is also included in the form of activation energies increments.

Isomerization reactions of radicals, transferring the radical between positions 1 and 4, 1 and 5 or within allyl type radical is always considered to be bidirectional chemical reaction with the same kinetic parameters on both sides, parameters that are typical for the type of isomerization but independent of radical structure.

If there is a radical that cannot be stabilized by decomposition reactions and cannot be transformed by any isomerization leading to stabilization, it is terminated in recombination reaction by hydrogen radical. Frequency factor and activation energy are typical for each type of these reactions. Complete list of generalized kinetic parameters (factors of the group contribution method) is provided in Table 3 and the details on the group contribution method are available in our earlier papers [37,52].

These set of primary pyrolysis reactions was supplemented by a set of chemical reactions replacing hydrogenation, radical addition, isomerization and scission of components containing from 1 to 4 carbon atoms, as well as the aromatization reactions. The parameters were adopted from the earlier work [37] and the parameters are summarized in Table 2.

The reactors are modeled as straight, isobaric reactors with plug-flow of the reaction mixture. The temperature of the reaction mixture is provided by measured temperature profiles as the rate of heat transfer would be much faster than the heat consumption by chemical reactions.

Mass balance of reaction component *i* along the reactor is given by Eq. (1)

$$\frac{dJ_i}{dz} = \sum_j r_j \nu_{j,i} \tag{1}$$

where J is the molar flow density, z is length coordinate, r_j is rate of jth reaction, and $\nu_{j,i}$ is a stoichiometric coefficient of the ith component in the jth reaction. Temperature profile is described by the polynomial function of z and the derivatives of that expression can be easily obtained analytically. Reaction rates are assumed being of the first order to each reactant. In hydrogen abstraction reaction, the virtual active radical activity takes place of one of the reactants.

$$r_j = k_j \prod_{i \in I_j} c_i \quad \text{or} \quad r_j = a_{actR} \cdot k_j \prod_{i \in I_j} c_i \tag{2}$$

where k_j is the rate constant of jth reaction, c_i is the concentrations of reaction educts taken from the set of reaction educts I_j and a_{actR} is the total activity of active radicals.

Rate constants are determined from Arrhenius equation using estimated kinetic parameters as it was explained above. Reaction components are assumed to conform to the ideal gas state behavior.

The initial values of the group contribution factors were set up, so that the resulting kinetic parameters were close to the values reported in the literature. The factors were then optimized [35] for the model to be fitting the experimental data obtained on the reactor system A (see Table 1). The data set used for the optimization included several structurally different hydrocarbons (n-heptane, 2-methylheptane, 2,2-dimethylheptane, 2,4-dimethylheptane, cyclopentane, cyclohexane, methylcyclohexane, 1,2-dimethylcyclohexane) at different temperatures and residence times. Weighted sum of squares of errors between the simulated and experimental values of components weight fractions in the product stream was used as the objective function. Weights were set up so as to reflect both the relative and absolute component of the experimental error. Owing to the difficult computation of high-precision results, the usage of derivatives-using optimization methods was inefficient. Therefore, we used the adaptive random search method which already proved being able to provide satisfactory performance [1,53]. Additionally, when any base activating energy factor change was tried during an iteration of optimization process, related frequency factor was recalculated automatically in order to preserve the absolute value of kinetic constant at typical process temperature. Therefore, the iteration tested mainly the change of the rate constant sensitivity to temperature, not its value at typical reaction temperature. The frequency factor value was adjusted by separate algorithm during the iteration. This improvement of the optimizing method highly increased the proportion of successful iterations and the method convergence rate as it alleviated the problem of activation energy/frequency factor correlation.

3. Results and discussion

The model described in the previous section, using the original parameters listed in Table 3, was used to simulate the experiments on n-heptane cracking, carried out in different reactors. The experimental setups and the comparison of simulated and experimental n-heptane conversions are provided in Table 4. Simulations performed for reactor A generated reasonably good predictions of n-heptane conversion, non-surprisingly, as the original model parameters were based on experiments carried out in this reactor. The results for reactor B were substantially less accurate, especially at higher conversions. It is partially due to the quite different properties of the reactor B, especially the wall material, steam dilution and mode of operation, but for most part we believe it was caused by the limited accuracy of the temperature profile measurement in the reactor A, due to its very small size.

The results indicate the model only partially generalize the kinetics of pyrolysis reactions. Actually the experimental data of reactor A are rather “over-fitted”, i.e. the model describes not only the real relationships between the operating parameters and the product yields, but also corrects some part of systematic error present in the experimental data. The behavior is not surprising, since it is a general trend in parameter-rich models. It generally results in the important kinetic parameters varying significantly among different authors [54–58], depending on the experimental conditions used.

In order to improve the model, we included the data measured on significantly different reactor B at quite different conditions into the parameter optimization process of our model development. The data set included the experiments carried out in the reactor

Table 3
Parameters of group contribution method for estimating the kinetic parameters of pyrolysis reactions based on the data from the pulse reactor (original = before generalization) and from both the pulse and continuous reactor (improved = after generalization) (frequency factors [A] = s^{-1}, $m^3\ mol^{-1}\ s^{-1}$, activating energies [E] = [ΔE] = $kJ\ mol^{-1}$).

Parameter	Reaction template	Parameter values	
		Original	Improved
A	H-abstraction	7.9×10^{12}	7.0×10^{12}
E	H-Abstraction on primary carbon	95.1	92.4
E	H-Abstraction on secondary carbon	93.2	92.4
E	H-Abstraction on tertiary carbon	84.5	81.2
ΔE[a]	H-Abstraction (allylic position modifier)	−6.5	−7.7
A	β-Scission C—C (aliphatic bond)	1.5×10^{13}	7.3×10^{12}
A	β-Scission C—C (carbocycle bond)	9.3×10^{9}	
E	β-Scission C—C (1 alkyl)	190.9	199.0
E	β-Scission C—C (2 alkyl)	142.4	105.7
E	β-Scission C—C (3 alkyl)	97.1	97.6
E	β-Scission C—C (4 alkyl)	84.7	90.3
A	β-Scission C—H	2.6×10^{08}	1.8×10^{10}
E	β-Scission C—H (primary carbon)	145.7	184.8
E	β-Scission C—H (secondary carbon)	110.3	163.2
E	β-Scission C—H (tertiary carbon)	55.1	123.2
ΔE	β-Scission (multiple bond in β position modifier)	−9.0	−5.7
A	Recombination	1.0×10^{10}	1.0×10^{10}
E	Recombination	0.0	0.0
A	Allyl isomerization	4.0×10^{12}	2.5×10^{18}
E	Allyl isomerization	144.8	144.8
A	1,4-Isomerization	1.7×10^{12}	37.7
E	1,4-Isomerization	168.0	220.7
A	1,5-Isomerization	1.1×10^{13}	9.1×10^{05}
E	1,5-Isomerization	168.0	171.8
A	Reverse Diels–Alder reaction	8.2×10^{15}	
E	Reverse Diels–Alder reaction	271.3	

[a] ΔE is a modifier to the value of any E of the same type where appropriate.

A for representing the hydrocarbon structure variability and it was expanded by results of six experimental runs of n-heptane pyrolysis carried out in the reactor B (runs 3–8 in Table 5). The model was then optimized by the same optimization procedure described above. Only the parameters playing a significant role in n-heptane cracking were optimized in this step. Resulting parameters from this optimization step are shown in the last column of Table 3. There are slight changes in hydrogen abstraction parameters responsible for simulating the relationships between the temperature, residence time, and conversion more accurately over a broader range of experimental conditions. However, there are also substantial changes in parameters, the effect of which on the kinetics of n-heptane cracking should be negligible, such as the activating energies of β-scission of 4-alkyl-substituted C—C bond or β-scission of C—H bond on tertiary carbon atom. Compounds being eligible undergoing such reactions may occur in the reaction mixture only as products and thus those reactions should be of secondary importance. However, there should be stressed that 2-methylheptane, 2,2-dimethylheptane, 2,4-dimethylheptane, cyclopentane, cyclohexane, methylcyclohexane, 1,2-dimethylcyclohexane simulations data were left in the data set for optimization. Thus, the change of the kinetic parameters of those reactions acts as compensation to the changes in other parameters important for n-heptane cracking. Thus, the inclusion of the n-heptane data from different experimental setup, improves not only the simulation of n-heptane cracking, but improves also the reliability of the model simulations for different hydrocarbon structures.

The improved predictions of n-heptane conversion after the generalization step are provided in Table 4 for comparison. The prediction error is smaller and much more evenly distributed among different experimental runs. The more detailed results are shown in Table 5, which provide the comparison of simulated and experimental data for 11 experimental runs, carried out in the different reactors. There are also simulations of validation runs provided to show the model performance on simulating experiments not being a part of the optimization process. Simulated data correspond to the experiments very well at lower conversions, however at higher conversions, the differences are more significant. This is probably due to the more significant impact of secondary reactions (reactions involving the first-generation alkenes, namely condensation reactions) at higher conversions. Since the secondary reactions are modeled by relatively simplified system of molecular reactions, the modeling results are less accurate in such cases.

The graphical comparison of calculated and experimental profiles of conversion is shown in Fig. 2. The improved model predicts the n-heptane conversion accurately for different temperature

Table 4
Comparison of experimental conversions of n-heptane at selected reaction conditions and those simulated by the model before and after the generalization step.

Reactor	T_{max}, °C	F, mg s^{-1}	Ratio (H_2O/C_7)	x_{C7}, %		
				Sim. original	Sim. improved	Exp.
A	700	10.2	0.0	7.2	7.8	7.2
A	815	6.8	0.0	85.9	88.8	87.7
B	680	9.5	3.1	4.0	4.7	4.8
B	680	4.2	3.1	8.8	10.3	10.5
B	760	6.7	3.0	36.7	41.3	42.8
B	720	9.7	2.9	11.2	13.1	11.2
B	720	4.2	3.0	24.2	27.9	29. 8
B	760	9.9	3.0	26.7	30.5	28.1

Table 5
Comparison of experimental and simulated conversion of n-heptane and composition of the product stream for various reaction conditions.

Run	1		2		3		4		5		6		7		8		9		10		11		12	
Reactor	A		A		B		B		B		B		B		B		B		B		B		A	
T_{max}, °C	700		815		680		680		760		720		720		760		700		700		720		815	
F, mg s^{-1}	10.24		6.83		9.46		4.16		6.96		9.68		4.16		9.91		9.81		4.16		6.78		10.24	
Ratio (H_2O/C_7)	0.00		0.00		3.11		3.06		3.02		2.94		3.03		2.96		3.01		2.97		3.06		0.00	
t_R, s	0.493		0.356		0.202		0.462		0.257		0.200		0.448		0.186		0.20		0.47		0.27		0.493	
Type[a]	O		O		O		O		O		O		O		O		V		V		V		V	
	Exp.	Sim.	Exp.	Sim.	Exp.	Sim.	Exp.	Sim.	Exp.	Sim.	Exp.	Sim.	Exp.	Sim.	Exp.	Sim.	Exp.	Sim.	Exp.	Sim.	Exp.	Sim.	Exp.	Sim.
Conversion	7.2	7.8	87.7	88.8	4.8	4.7	10.5	10.3	42.8	41.3	11.2	13.1	29.8	27.9	28.1	30.5	6.1	7.8	16.8	17.7	16.0	17.8	93.2	93.2
Product composition, wt.%																								
Hydrogen	0.14	0.07	0.88	0.93	0.02	0.04	0.06	0.10	0.22	0.42	0.07	0.12	0.17	0.28	0.16	0.30	0.03	0.07	0.11	0.17	0.10	0.17	0.75	0.81
Methane	0.39	0.48	7.13	7.90	0.44	0.26	1.00	0.62	3.29	2.92	0.94	0.83	2.46	1.86	2.10	2.11	0.57	0.46	1.38	1.13	1.33	1.15	9.88	8.64
Ethane	0.10	0.03	2.11	2.15	0.20	0.00	0.50	0.00	0.98	0.01	0.33	0.00	0.81	0.01	0.63	0.00	0.25	0.00	0.50	0.00	0.45	0.00	4.11	1.30
Ethylene	2.65	3.24	48.08	44.94	2.19	1.82	5.28	4.29	19.98	19.30	5.33	5.51	14.31	12.59	12.85	13.84	3.10	3.15	7.77	7.69	7.60	7.68	45.87	47.03
Propane	0.03	0.00	0.53	0.00	0.03	0.00	0.10	0.00	0.25	0.00	0.05	0.00	0.17	0.00	0.16	0.00	0.03	0.00	0.08	0.00	0.08	0.00	0.67	0.00
Propylene	1.11	1.44	15.34	13.55	0.73	0.84	2.17	1.92	8.38	7.27	2.07	2.33	6.11	5.08	5.26	5.34	1.19	1.40	3.14	3.27	3.04	3.20	16.62	14.00
Acetylene	0.00	0.00	0.57	0.00	0.00	0.00	0.00	0.00	0.06	0.00	0.00	0.00	0.02	0.00	0.03	0.00	0.00	0.00	0.00	0.00	0.01	0.00	0.40	0.00
Propyne	0.00	0.00	0.34	0.00	0.00	0.00	0.00	0.00	0.03	0.00	0.00	0.00	0.01	0.00	0.01	0.00	0.00	0.00	0.00	0.00	0.00	0.00	0.15	0.00
n-Butane	0.00	0.00	0.01	0.00	0.01	0.00	0.04	0.00	0.05	0.00	0.01	0.00	0.04	0.00	0.03	0.00	0.01	0.00	0.02	0.00	0.02	0.00	0.14	0.00
Isobutane	0.01	0.00	0.23	0.00	0.00	0.00	0.00	0.00	0.00	0.00	0.00	0.00	0.00	0.00	0.00	0.00	0.00	0.00	0.00	0.00	0.00	0.00	0.02	0.00
1-Butene	0.98	0.99	5.10	5.43	0.31	0.62	1.00	1.30	4.52	4.55	1.06	1.66	3.22	3.24	2.93	3.59	0.60	1.02	1.60	2.16	1.61	2.19	3.85	6.19
2-Butene	0.01	0.07	0.49	0.59	0.00	0.03	0.03	0.10	0.11	0.41	0.01	0.10	0.07	0.31	0.05	0.27	0.01	0.05	0.02	0.19	0.02	0.16	0.55	0.62
Isobutene	0.00	0.00	0.08	0.00	0.00	0.00	0.00	0.00	0.02	0.00	0.00	0.00	0.01	0.00	0.01	0.00	0.00	0.00	0.00	0.00	0.00	0.00	0.11	0.00
Butadienes	0.04	0.01	4.21	5.54	0.02	0.00	0.08	0.02	0.92	0.51	0.08	0.03	0.44	0.20	0.44	0.24	0.04	0.01	0.15	0.07	0.15	0.07	4.96	7.12
C_5-C_6 NA	1.65	0.67	2.09	4.68	0.45	0.40	0.21	0.88	2.86	3.19	0.71	1.11	1.28	2.26	2.47	2.45	0.23	0.67	2.00	1.48	1.55	1.48	2.17	4.80
Benzene	0.06	0.00	0.38	0.46	0.00	0.00	0.00	0.00	0.00	0.00	0.00	0.00	0.00	0.00	0.00	0.00	0.00	0.00	0.00	0.00	0.00	0.00	1.19	0.19
Toluene	0.00	0.00	0.06	0.07	0.00	0.00	0.00	0.00	0.00	0.00	0.00	0.00	0.00	0.00	0.00	0.00	0.00	0.00	0.00	0.00	0.00	0.00	0.32	0.03
Unlisted	0.00	0.78	0.06	2.49	0.41	0.66	0.06	1.10	1.18	2.66	0.57	1.39	0.67	2.05	1.02	2.38	0.00	0.96	0.00	1.53	0.00	1.70	0.90	0.00

[a] O = used for optimization; V = used for validation.

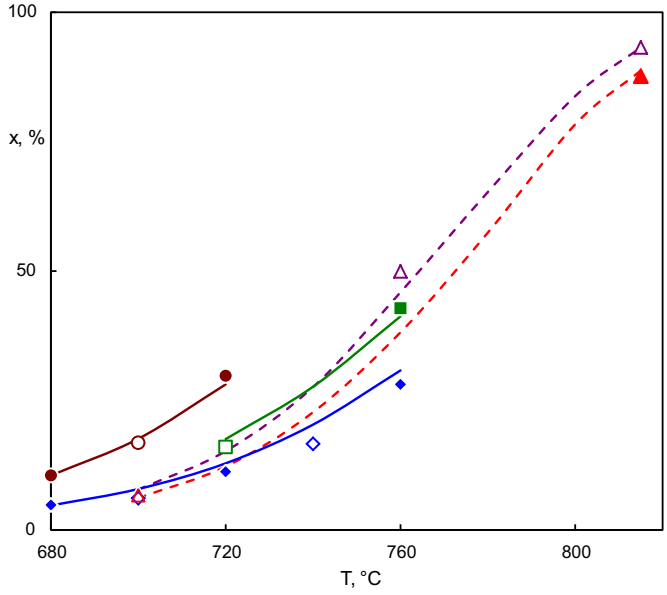

Fig. 2. Comparison of experimental (points) and simulated (lines) conversions of n-heptane at different temperatures and residence times (temperature indicates the peak temperature in the reactor) Reactor A (dashed lines) t_R = ▲ 0.356 s, ▼ 0.493 s Reactor B (solid lines) t_R = ● 0.45–0.47 s, ■ 0.26 s and ◆ 0.19–0.20 s filled points were included in optimization process, empty points represent the validation data.

profiles, pressure, dilution ratio, and reactor type. There may be slight systematic deviation between some predictions and the experimental data, but it corresponds to the wide range of the operating parameters, that are modeled. The validation points are fitted equally well as the points used in the regression, therefore indicating very robust prediction. In addition, one can notice there are mainly validation points for the reactor A displayed in the figure. Therefore, it may be concluded our objective to develop the model able to predict the conversion profiles in reactor A based on the detailed data from reactor B, was successfully achieved.

Fig. 3 shows the comparison of simulated product yields profiles and the experimental data. Again, the ethylene yields are predicted by the model quite well, regardless of the reactor type or operating parameters. Good predication by the model is valid also for other products, but only within the temperature range 680–760 °C. Above 760 °C, i.e. at conversions above 60%, the propylene and methane yields are significantly underestimated, while the C4 yields are overestimated by the model. It is due to the simplified approach adopted to describe the secondary radical addition reactions (discussed above). The substitute molecular reactions are good enough approach for modeling the secondary reactions in a single compound pyrolysis carried out in one reactor type as we observed in our earlier papers as well as it was reported by other authors, but in generalized model, they are responsible for somewhat worse simulation of some product yields in high-conversion experiments.

It is very difficult to compare values of kinetic parameters directly with other researchers due to significantly different modeling approach. Several models contain detailed description of hydrogen abstraction by rich set of radicals and others by much more limited set of radicals, in opposite to our approach where an abstract active radical is considered. Moreover, in several models all chemical reactions are considered to be reversible, others consider reversibility only partially, unlike others, including our model, where the reversibility is taken into account only for selected reactions. In addition, some papers utilize extended Arrhenius equation even with pressure-dependence of kinetic parameters. However, the values of kinetic parameters may be compared to those obtained by other researchers in terms of general trends in kinetic parameters of several reaction types. The activation energies of C—H scission on primary carbon atom are higher than scission of C—H bonds on secondary carbon, in accordance to values reported for C6 radical [19,59] or C4 radicals [60,61]. Scission of terminating C—C bonds in linear radicals is slower than scission of non-terminating ones in the same cases. The presence of double bond in the alpha position to the bond which undergoes the scission causes increasing of activation energy and the presence of double bond in beta position causes decrease. Activation energies of C—H scission are higher than C—C scission and the relative values of discussed changes in activation are approximately similar.

The model generalization can be evaluated on the data from control simulations shown in Table 6. The simulations are compared to the experimental data obtained in reactor A at the similar

Table 6
Comparison of experimental and simulated yields of validation hydrocarbons in reactor A.

Feed	2-Methylheptane				2,4-Dimethylpentane			
T_{max}, °C	700		815		700		815	
t_R, s	0.475		0.329		0.368		0.363	
	Exp.	Sim.	Exp.	Sim.	Exp.	Sim.	Exp.	Sim.
Conversion	12.4	13.2	94.0	95.8	10.3	11.6	93.0	98.2
Product composition, wt.%								
Hydrogen	0.24	0.00	0.89	0.84	0.19	0.06	0.80	0.74
Methane	0.62	2.80	9.02	9.93	0.52	1.16	11.75	14.68
Ethane	0.27	0.00	2.18	1.23	0.07	0.00	1.13	0.17
Ethylene	2.94	3.26	34.24	30.61	0.17	0.00	9.85	5.30
Propane	0.07	0.00	0.53	0.00	0.02	0.00	0.52	0.00
Propylene	2.74	2.59	22.22	25.82	3.97	4.61	36.60	43.73
Acetylene	0.01	0.00	0.49	0.00	0.00	0.00	0.44	0.00
Propyne	0.01	0.00	0.63	0.00	0.04	0.00	0.84	0.00
n-Butane	0.00	0.00	0.01	0.00	0.00	0.00	0.01	0.00
Isobutane	0.02	0.00	0.59	0.00	0.05	0.00	1.04	0.00
1-Butene	0.68	0.83	3.55	5.42	0.06	0.78	3.47	7.02
2-Butene	0.04	0.06	0.76	0.53	0.01	0.04	0.72	0.69
Isobutene	1.65	0.25	6.08	1.48	3.21	1.63	13.39	2.23
Butadienes	0.08	0.04	5.38	7.52	0.03	0.00	3.62	6.66
C_5-C_6 NA	2.35	1.03	4.38	6.04	1.84	2.14	5.75	13.80
Benzene	0.10	0.00	1.13	0.41	0.04	0.00	1.45	0.06
Toluene	0.17	0.00	0.52	0.17	0.00	0.00	0.85	0.27
Unlisted	0.41	1.46	1.45	3.24	0.03	0.00	0.71	0.02

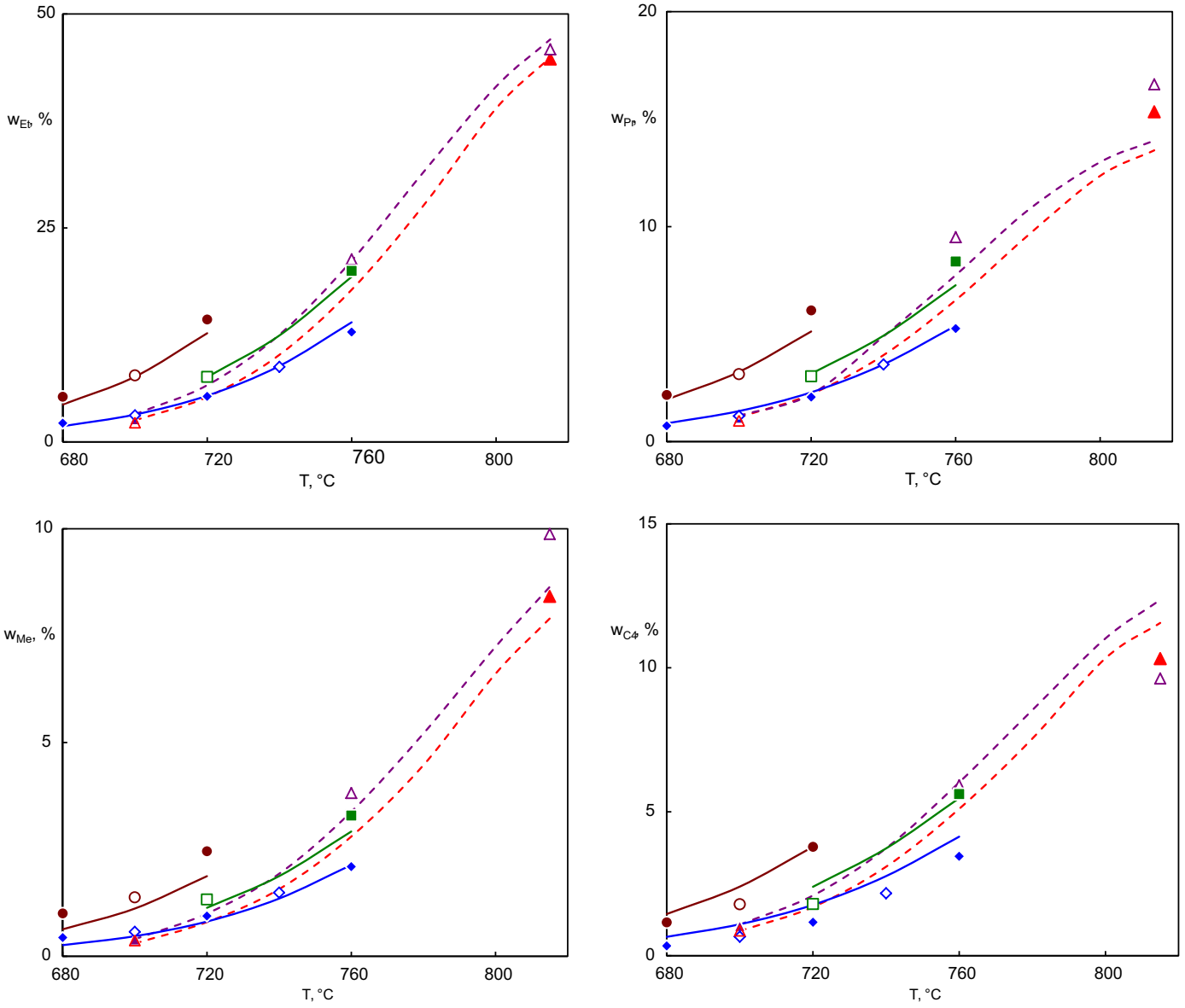

Fig. 3. Comparison of experimental (points) and simulated (lines) mass fraction of ethylene, propylene, methane, and C4-fraction in product of n-heptane cracking at different temperature and residence time Reactor A (dashed lines) t_R = ▲ 0.356 s, ▼ 0.493 s Reactor B (solid lines) t_R = ● 0.45–0.47 s, ■ 0.26 s and ◆ 0.19–0.20 s filled points were included in optimization process, empty points represent the validation data.

reaction conditions to heptane experiments. Comparing the experimental and simulated data of those validation experiments shows our effort to improve the generalization of the model was at least partially successful. The deviations between the simulated and experimental conversions are only slightly higher for control hydrocarbons than those for n-heptane. The same is true for product composition, at least for the low-conversion experiments. At high-conversion experiments, the predictions are somewhat more deviated from the experimental data, especially for the C_4^+ fraction products, involved in secondary reactions.

4. Conclusions

In this work, the mathematical model of pyrolysis reactions employing the automated reaction network generation was successfully applied on combined data comprising the experimental results of n-heptane pyrolysis carried out under broad range of experimental conditions and the experimental data of pyrolysis of several structurally different hydrocarbons, carried out under constant experimental condition. The model was able to fit all the data set simultaneously providing an improved generalization of n-heptane pyrolysis reaction kinetics. The model is able to predict the n-heptane conversion accurately at different temperature, pressure, residence time, dilution ratio, and reactor type. The product yields are simulated very accurately up to 760 °C, while at higher temperatures, i.e. for higher n-heptane conversion, the results are somewhat less accurate due to the simplified approach used for modeling the secondary reactions. There is however a great potential for further improvement of the model by using ARNG approach for modeling secondary reactions as well, since the generalization procedure itself, based on using combined data was proved very successful.

Acknowledgements

Financial support by Ministry of Education Youths and Sports of the Czech Republic (Specific university research MSMT No.

20/2013) and VEGA Scientific Grant Agency of the Slovak Republic (the Research project No. 1/0228/12) is gratefully acknowledged

References

[1] Z. Belohlav, P. Zamostny, T. Herink, The kinetic model of thermal cracking for olefins production, Chem. Eng. Process. 42 (2003) 461–473.
[2] Z. Bělohlav, P. Zámostný, E. Eckert, T. Vaněk, T. Herink, Evaluation of atmospheric gas oil properties through the laboratory and simulated pyrolysis, in: 17th International Congress of Chemical and Process Engineering, P7.77, Prague, 2006, pp. 1–6.
[3] J. Doskocil, Z. Belohlav, T. Herink, P. Zamostny, Improvement of pyrolysis reactors in Chemopetrol Co. Litvinov, Chem. Listy 97 (2003) 1176–1180.
[4] T. Herink, Z. Belohlav, P. Zamostny, J. Doskocil, Application of hydrocarbon cracking experiments to ethylene unit control and optimization, Petrol. Chem. 46 (2006) 237–245.
[5] T. Herink, Z. Belohlav, P. Zamostny, J. Doskocil, J. Lederer, P. Svoboda, Complex research of hydrocarbon pyrolysis in the chemopetrol litvinov plant, Chem. Listy 99 (2005) 443–446.
[6] A. Karaba, P. Zamostny, T. Herink, J. Lederer, Using the semi-mechanistic steam-cracking model to improve steam-cracker operation, Procedia Eng. 42 (2012) 2131–2139.
[7] K.K. Pant, D. Kunzru, Pyrolysis of n-heptane: kinetics and modeling, J. Anal. Appl. Pyrolysis 36 (1996) 103–120.
[8] L. Tian, J. Wang, B. Shen, J. Liu, Building a kinetic model for steam cracking by the method of structure-oriented lumping, Energy Fuels 24 (2010) 4380–4386.
[9] K.M. Sundaram, G.F. Froment, Modeling of thermal cracking kinetics II. Cracking of iso-butane, of n-butane and of mixtures ethane–propane–n-butane, Chem. Eng. Sci. 32 (1977) 609–617.
[10] K.M. Sundaram, G.F. Froment, Modeling of thermal cracking kinetics. I. Thermal cracking of ethane, propane and their mixtures, Chem. Eng. Sci. 32 (1977) 601–608.
[11] D.L. Allara, R. Shaw, A compilation of kinetic parameters for the thermal degradation of n-alkane molecules, J. Phys. Chem. Ref. Data 9 (1980) 523–559.
[12] K.M. Sundaram, G.F. Froment, Two dimensional model for the simulation of tubular reactors for thermal cracking, Chem. Eng. Sci. 35 (1980) 364–371.
[13] E. Ranzi, M. Dente, S. Pierucci, G. Biardi, Initial product distributions from pyrolysis of normal and branched paraffins, Ind. Eng. Chem. Fundam. 22 (1983) 132–139.
[14] D. Depeyre, C. Flicoteaux, Modeling of thermal steam cracking of N-hexadecane, Ind. Eng. Chem. Res. 30 (1991) 1116–1130.
[15] M.F.P. Di, P.G. Lignola, King, a kinetic network generator, Chem. Eng. Sci. 47 (1992) 2713–2718.
[16] L.J. Broadbelt, S.M. Stark, M.T. Klein, Computer-generated pyrolysis modeling – on-the-fly generation of species, reactions, and rates, Ind. Eng. Chem. Res. 33 (1994) 790–799.
[17] D. Matheu, A.M. Dean, J.M. Grenda, Pressure-dependent automated mechanism generation for high-conversion ethane pyrolysis, Abstr. Pap. Am. Chem. Soc. 228 (2004) U223.
[18] K.M. Van Geem, Single event microkinetic modeling for steam cracking of hydrocarbons (PhD dissertation), Universiteit Gent, Gent, 2006.
[19] K.M. Van Geem, M.F. Reyniers, G.B. Marin, J. Song, W.H. Green, D.M. Matheu, Automatic reaction network generation using RMG for steam cracking of n-hexane, AIChE J. 52 (2006) 718–730.
[20] K.M. Van Geem, G.J. Heynderickx, G.B. Marin, Effect of radial temperature profiles on yields in steam cracking, AIChE J. 50 (2004) 173–183.
[21] K.M. Van Geem, M.-F. Reyniers, G.B. Marin, J. Song, W.H. Green, D.M. Matheu, Automatic reaction network generation using RMG for steam cracking of n-hexane, AIChE J. 52 (2006) 718–730.
[22] W. Sun, M. Saeys, Construction of an ab initio kinetic model for industrial ethane pyrolysis, AIChE J. 57 (2011) 2458–2471.
[23] D.M. Matheu, J.M. Grenda, A systematically generated, pressure-dependent mechanism for high-conversion ethane pyrolysis. 1. Pathways to the minor products, J. Phys. Chem. A 109 (2005) 5332–5342.
[24] P.A. Willems, G.F. Froment, Kinetic modeling of the thermal cracking of hydrocarbons. 1. Calculation of frequency factors, Ind. Eng. Chem. Res. 27 (1988) 1959–1966.
[25] L.J. Broadbelt, S.M. Stark, M.T. Klein, Computer generated pyrolysis modeling: on-the-fly generation of species, reactions, and rates, Ind. Eng. Chem. Res. 33 (1994) 790–799.
[26] T.M. Perumal, S. Madgula Krishna, S.S. Tallam, R. Gunawan, Reduction of kinetic models using dynamic sensitivities, Comput. Chem. Eng. 56 (2013) 37–45.
[27] H. Huang, M. Fairweather, J. Griffiths, A. Tomlin, R. Brad, A systematic lumping approach for the reduction of comprehensive kinetic models, Proc. Combust. Inst. 30 (2005) 1309–1316.
[28] I.P. Androulakis, Kinetic mechanism reduction based on an integer programming approach, AIChE J. 46 (2000) 361–371.
[29] K. Edwards, T. Edgar, V. Manousiouthakis, Reaction mechanism simplification using mixed-integer nonlinear programming, Comput. Chem. Eng. 24 (2000) 67–79.
[30] A. Mitsos, G.M. Oxberry, P.I. Barton, W.H. Green, Optimal automatic reaction and species elimination in kinetic mechanisms, Combust. Flame 155 (2008) 118–132.
[31] S.W. Benson, Methods for the Estimation of Thermochemical Data and Rate Parameters, John Wiley & Sons, New York, 1976.
[32] S. Raman, H.-H. Carstensen, Tree structure for intermolecular hydrogen abstraction from hydrocarbons (C/H) and generic rate constant rules for abstraction by vinyl radical, Int. J. Chem. Kinet. 44 (2012) 327–349.
[33] A. Karaba, P. Zamostny, Simplifying complex computer-generated reactions network to suppress its stiffness, Procedia Eng. 42 (2012) 1773–1782.
[34] A. Karaba, P. Zamostny, Z. Belohlav, Modelling steam-cracking kinetics by the computer-generated network of reactions, in: 19th International Congress of Chemical and Process Engineering (CHISA), Prague, CZ, 2010, p. 7.
[35] A. Karaba, P. Zamostny, T. Herink, J. Lederer, Using the semi-mechanistic steam-cracking model to improve steam-cracker operation, in: P. Kluson (Ed.), 20th International Congress of Chemical and Process Engineering, Prague, CZ, 2012.
[36] P. Zamostny, Z. Belohlav, L. Starkbaumova, J. Patera, Experimental study of hydrocarbon structure effects on the composition of its pyrolysis products, J. Anal. Appl. Pyrolysis 87 (2010) 207–216.
[37] A. Karaba, P. Zamostny, J. Lederer, Z. Belohlav, Generalized model of hydrocarbons pyrolysis using automated reactions network generation, Ind. Eng. Chem. Res. 52 (2013) 15407–15416.
[38] M. Bajus, V. Vesely, Hydrocarbon pyrolysis. I. Pyrolysis of individual N-alkanes, Ropa Uhlie 18 (1976) 126–135.
[39] M. Bajus, V. Vesely, P.A. Leclercq, J.A. Rijks, Steam cracking of hydrocarbons. 1. Pyrolysis of heptane, Ind. Eng. Chem. Prod. Res. Dev. 18 (1979) 30–37.
[40] N. Olahová, M. Bajus, E. Hájeková, L. Šugár, J. Markoš, Kinetics and modelling of heptane steam-cracking, Chem. Pap. (2013) 1–12.
[41] W.G. Appleby, W.H. Avery, W.K. Meerbott, Kinetics and mechanism of the thermal decomposition of heptane, J. Am. Chem. Soc. 69 (1947) 2279–2285.
[42] M. Murata, S. Saito, A. Amano, S. Maeda, Prediction of initial product distributions from pyrolysis of normal paraffinic hydrocarbons, J. Chem. Eng. Jap. 6 (1973) 252–258.
[43] M. Murata, S. Saito, Prediction of initial product distribution from normal paraffin pyrolysis at higher temperatures by considering ethyl radical decomposition, J. Chem. Eng. Jpn. 7 (1974) 389–391.
[44] M. Murata, S. Saito, Simulation model for high-conversion pyrolysis of normal paraffinic hydrocarbons, J. Chem. Eng. Jpn. 8 (1975) 39–45.
[45] M. Bajus, V. Vesely, P.A. Leclercq, J.A. Rijks, Steam cracking of hydrocarbons. 1. Pyrolysis of heptane, Ind. Eng. Chem. Prod. Res. Dev. 18 (1979) 30–37.
[46] D.S. Aribike, A.A. Susu, Mechanistic modeling of the pyrolysis of n-heptane, Thermochim. Acta 127 (1988) 259–273.
[47] D.S. Aribike, A.A. Susu, Kinetics and mechanism of the thermal cracking of n-heptane, Thermochim. Acta 127 (1988) 247–258.
[48] J.P. Chakraborty, D. Kunzru, High pressure pyrolysis of n-heptane, J. Anal. Appl. Pyrolysis 86 (2009) 44–52.
[49] P. Zamostny, Z. Belohlav, L. Starkbaumova, A Multipurpose micro-pulse reactor for studying gas-phase reactions, Chem. Biochem. Eng. Q. 21 (2007) 105–113.
[50] E. Hajekova, M. Bajus, Recycling of low-density polyethylene and polypropylene via copyrolysis of polyalkene oil/waxes with naphtha: product distribution and coke formation, J. Anal. Appl. Pyrolysis 74 (2005) 270–281.
[51] E. Hajekova, B. Mlynkova, M. Bajus, L. Spodova, Copyrolysis of naphtha with polyalkene cracking products; the influence of polyalkene mixtures composition on product distribution, J. Anal. Appl. Pyrolysis 79 (2007) 196–204.
[52] A. Karaba, P. Zamostny, Simplifying complex computer-generated reactions network to suppress its stiffness, Procedia Eng. 42 (2012) 1773–1782.
[53] Z. Belohlav, P. Zamostny, P. Kluson, J. Volf, Application of random-search algorithm for regression analysis of catalytic hydrogenations, Can. J. Chem. Eng. 75 (1997) 735–742.
[54] J. Ding, L. Zhang, K. Han, Thermal rate constants of the pyrolysis of n-heptane, Combust. Flame 158 (2011) 2314–2324.
[55] T. Yuan, L. Zhang, Z. Zhou, M. Xie, L. Ye, F. Qi, Pyrolysis of n-heptane: experimental and theoretical study, J. Phys. Chem. A 115 (2011) 1593–1601.
[56] S. Garner, R. Sivaramakrishnan, K. Brezinsky, The high-pressure pyrolysis of saturated and unsaturated C7 hydrocarbons, Proc. Combust. Inst. 32 (2009) 461–467.
[57] J.P. Chakraborty, D. Kunzru, High-pressure pyrolysis of n-heptane: effect of initiators, J. Anal. Appl. Pyrolysis 95 (2012) 48–55.
[58] V.R. Katta, S.K. Aggarwal, W.M. Roquemore, Evaluation of chemical-kinetics models for n-heptane combustion using a multidimensional CFD code, Fuel 93 (2012) 339–350.
[59] D. Depeyre, C. Flicoteaux, Modeling of thermal steam cracking of normal-hexadecane, Ind. Eng. Chem. Res. 30 (1991) 1116–1130.
[60] M. Dente, E. Ranzi, A.G. Goossens, Detailed prediction of olefin yields from hydrocarbon pyrolysis through a fundamental simulation-model (Spyro), Comput. Chem. Eng. 3 (1979) 61–75.
[61] P.A. Willems, G.F. Froment, Kinetic modeling of the thermal cracking of hydrocarbons. 2. Calculation of activation energies, Ind. Eng. Chem. Res. 27 (1988) 1966–1971.